Wideband Negative Permeability Metamaterial with Non-Foster Compensation of Parasitic Capacitance

Konrad Miehle, Thomas P. Weldon, Ryan S. Adams, Kasra Daneshvar
Department of Electrical and Computer Engineering
University of North Carolina at Charlotte
Charlotte, NC, USA
tpweldon@uncc.edu

***Abstract*—The analysis and simulation of negative effective permeability of a magnetic metamaterial is presented, including parasitic effects. Beyond known issues of non-Foster circuit stability, such parasitics can limit bandwidth improvement. Based on the analysis, ideal non-Foster elements are added to split rings to achieve broadband negative effective permeability while compensating parasitic effects. Results indicate that both a negative capacitance and negative inductance are needed to achieve negative permeability from 0.5 to 4.5 GHz.**

I. Introduction

Magnetic metamaterial unit cells are commonly narrowband and dispersive. However, the appropriate use of non-Foster elements can increase the bandwidth of metamaterials, in principle [1], [2]. Therefore, the present work addresses the deleterious effects of parasitic fringe capacitance on the bandwidth of a single split-ring resonator when loaded with ideal non-Foster circuit elements. Analysis of the parasitics leads to modified equations for effective permeability, and simulation results confirm the potential for significantly improved bandwidth. In addition, the following discussion focuses only on the bandwidth problem with ideal elements, necessarily deferring more complex issues of stability with practical circuit elements for future investigation. Notwithstanding these limitations, the following analysis and simulation results illustrate the importance of mitigating such parasitics.

II. Wideband Unit Cell with Parasitic Effect

For simplicity, a lossless single split-ring resonator (SSRR) is used to illustrate the influence of parasitic fringe capacitance on the effective permeability of the metamaterial when using non-Foster elements. Consider a SSRR as shown in Fig. 1 centered in a unit cell with dimensions l_x, l_y, l_z. The area of the SSRR is A_R and the incident magnetic field H_0 is parallel to the axis of the SSRR. Due to the change in the magnetic field, a voltage v_g appears across the gap of the ring The gap in the split-ring can be modeled as a capacitance C_g. The current i_r in the ring and through capacitance C_g is then

$$i_r = C_g \frac{dv_g}{dt} = -C_g \frac{d^2(\Phi_0 + \Phi_R)}{dt^2} = -\Phi_0 \frac{s^2 C_g}{1 + s^2 L_R C_g} \,, \quad (1)$$

where s is the Laplace complex angular frequency, $L_R = \Phi_R / i_r$ is self-inductance, $v_g = -d(\Phi_0 + \Phi_R)/dt$, Φ_0 is the incident magnetic flux, and Φ_R is the magnetic flux due to i_r.

The well-known result in (1) describes the conventional narrowband behavior of a SSRR, where the magnetic resonance frequency can be defined as $\omega_{om} = 1/\sqrt{L_R C_g}$.

Next, consider replacing gap capacitance C_g with a positive inductance L_g with reactance $X_L = j\omega L_g$. The ring current i_r then becomes

$$i_r = \frac{1}{L_g} \int v_g dt = -\frac{1}{L_g}(\Phi_0 + \Phi_R) = -\Phi_0 \frac{1}{L_g + L_R} \,. \quad (2)$$

Comparing (1) with (2), the current in the split-ring is now frequency independent and broadband behavior is possible with proper choice of inductance L_g.

In practice, however, capacitance C_g cannot be removed completely and some parasitic fringe capacitance C_{Fg} will remain. As a result, the equivalent circuit in the gap of the split-ring is now a parallel combination of inductance L_g and fringe capacitance C_{Fg}. Modifying (2) with C_{Fg} yields

$$i_r = i_{C_{Fg}} + i_{L_g} = C_{Fg} \frac{dv_g}{dt} + \frac{1}{L_g} \int v_g dt \,, \quad (3)$$

where $i_{C_{Fg}}$ is the current through fringe capacitance C_{Fg}, and i_{L_g} is the current through inductance L_g. Substituting $v_g = -d(\Phi_0 + \Phi_R)/dt$ in (3), taking the Laplace transform, and including self-inductance L_R yields

$$i_r = -\Phi_0 \frac{1 + s^2 C_{Fg} L_g}{L_R + L_g(1 + s^2 C_{Fg} L_R)} \,. \quad (4)$$

The result in (4) indicates that two resonance frequencies exist.

To find effective permeability, magnetic dipole moment is used. The current in the SSRR creates a magnetic dipole moment $m = i_r A_R$. The magnetization M is then the magnetic

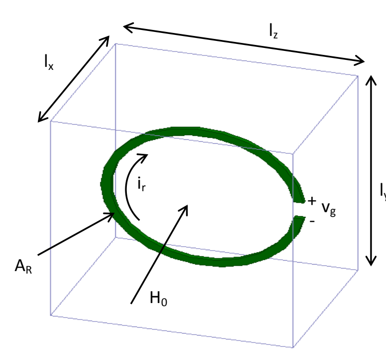

Fig. 1. Single split-ring resonator (SSRR) used as a example of a magnetic unit cell.

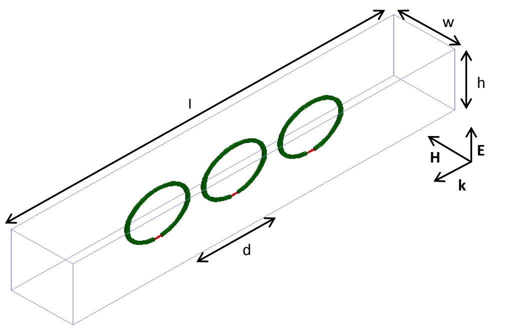

Fig. 2. Three SSRR (green) symmetric structure in parallel-plate waveguide. The radius of the SSRR rings are $4\,mm$, with gap of $1\,mm$, $d = 10\,mm$, $w = 10\,mm$, $h = 12\,mm$, $l = 50\,mm$.

dipole moment per unit volume, $M = (i_r A_R)/(l_x l_y l_z)$. Since $M = \chi_m H$, $\mu_r = 1 + \chi_m$, and $\Phi_0 = \mu_0 H_0 A_R$, the relative permeability, μ_r, equals

$$\mu_r = 1 - \mu_0 \frac{A_R^2}{l_x l_y l_z} \frac{1 - \omega^2 C_{Fg} L_g}{L_R + L_g(1 - \omega^2 C_{Fg} L_R)}, \quad (5)$$

where χ_m is the magnetic susceptibility, ω is the angular frequency, $\mu_\circ = 1.26 \times 10^{-6}$ H/m is the permeability of free space, and $s = j\omega$ was used.

Finally, the parasitic fringe capacitance C_{Fg} can theoretically be canceled by adding a parallel negative capacitance of equal value such that (5) becomes

$$\mu_r = 1 - \mu_0 \frac{A_R^2}{l_x l_y l_z} \frac{1}{L_R + L_g}, \quad (6)$$

and μ_r once again becomes frequency independent, making wideband negative effective permeability possible when L_g is negative, $L_R + L_g > 0$, and $L_R + L_g \approx 0$, according to (6).

III. Simulations

The metamaterial structure shown in Fig. 2 was simulated with three SSRR devices in a parallel-plate waveguide with perfect electric conductor top and bottom walls and with perfect magnetic conductor side walls. Three cases were simulated. The first case used conventional SSRR devices without non-Foster circuit elements. In the second case, all three SSRR devices were loaded with negative capacitance of -47 fF and negative inductance of -16.7 nH to confirm wideband behavior as predicted in (6). In the final case, the negative capacitance was removed and all three SSRR devices were only loaded with a negative inductance.

For the three cases simulated, S_{21} is plotted in Fig. 3 and extracted relative permeability is shown in Fig. 4 (using [3]). For both Figs. 3 and 4 the red solid and purple (circle) curves describe the conventional narrowband behavior. The magnetic resonance occurs near 2.5 GHz. The black dotted and dashed (square) curves illustrates wideband behavior from 0.5 to 4.5 GHz. The blue dashed and green (triangle) curves depict the result when the negative capacitance is removed.

IV. Conclusion

The deleterious effects of fringe capacitance were analyzed and found to strongly limit the bandwidth of negative effective

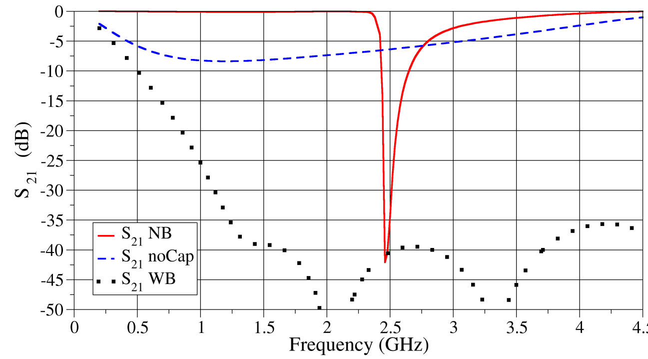

Fig. 3. Simulated S_{21} from structure shown in Fig. 2. The red solid curve shows narrowband behavior with conventional SRR. A 200 fF capacitance was added in the gap to create a resonance frequency near 2.5 GHz. The black dotted curve depicts wideband performance where SRR are loaded with ideal non-Foster elements and the blue dashed curve shows the result when negative capacitance is removed.

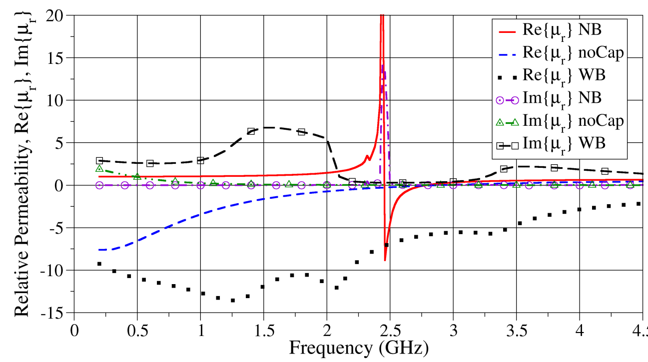

Fig. 4. Extracted real and imaginary parts of relative permeability for three cases. The red solid and purple dash-dot-dotted (circle) curves show conventional narrowband behavior with negative μ_r at resonance frequency. The black dotted and black dashed (square) curves illustrate wideband performance and the blue dashed and green dash-dotted (triangle) curves depict the behavior when negative capacitance is removed.

permeability in non-Foster loaded split ring resonators. The analysis and simulation results show that a non-Foster load with both negative inductance and negative capacitance is required for wideband behavior. Related results are in [4].

Acknowledgement

This material is based upon work supported by the National Science Foundation under Grant No. ECCS-1101939.

References

[1] S. Tretyakov, “Meta-materials with wideband negative permittivity and permeability,” *Microw. Opt. Technol. Lett.*, vol. 31, no. 3, pp. 163–165, 2001.

[2] S. Hrabar, I. Krois, I. Bonic, and A. Kiricenko, “Non-foster elements - new path towards broadband enz and mnz metamaterials,” in *Antennas and Propagation (EUCAP), Proceedings of the 5th European Conference on*, april 2011, pp. 2674–2677.

[3] Z. Szabo and, G.-H. Park, R. Hedge, and E.-P. Li, “A unique extraction of metamaterial parameters based on Kramers-Kronig relationship,” *Microwave Theory and Techniques, IEEE Transactions on*, vol. 58, no. 10, pp. 2646–2653, Oct 2010.

[4] T. P. Weldon, K. Miehle, R. S. Adams, and K. Daneshvar, “A wideband microwave double-negative metamaterial with non-Foster loading,” unpublished, submitted to IEEE SoutheastCon 2012.